Preprint typeset using LaTeX style emulateapj v. 12/16/11

FERMI BUBBLE γ-RAYS AS A RESULT OF DIFFUSIVE INJECTION OF GALACTIC COSMIC RAYS

Satyendra Thoudam
Department of Astrophysics, IMAPP, Radboud University Nijmegen
P.O. Box 9010, 6500 GL Nijmegen, The Netherlands

(Dated: April 26, 2013)

ABSTRACT

Recently, the *Fermi* space telescope has discovered two large γ-ray emission regions, the so-called "Fermi bubbles", that extend up to $\sim 50^\circ$ above and below the Galactic center. The γ-ray emission from the bubbles are found to follow a hard spectrum with no significant spatial variation in intensity and spectral shape. The origin of the emission is still not clearly understood. Suggested explanations include injection of cosmic-ray nuclei from the Galactic center by high-speed Galactic winds, electron acceleration by multiple shocks and stochastic electron acceleration inside the bubbles. In this letter, it is proposed that the γ-rays can be the result of diffusive injection of Galactic cosmic-ray protons during their propagation through the Galaxy. Considering that cosmic rays undergo much slower diffusion inside the bubbles than in the averaged Galaxy and at the same time suffer from inelastic collisions with the bubble plasma, this model can explain the observed intensity profile, the emission spectrum and the measured luminosity without invoking any additional particle production processes unlike other existing models.

Subject headings: cosmic rays — diffusion — Galaxy: halo — gamma rays: galaxies

1. INTRODUCTION

Recent detailed analysis of the *Fermi*-LAT data has discovered two giant γ-ray emission regions extending up to $\sim 50^\circ$ (~ 10 kpc) in Galactic latitude above and below the Galactic center with a width of $\sim 40^\circ$ in longitude (Su et al. 2010). The γ-ray emission regions, now popularly known as the "Fermi bubbles", coincide well with the WMAP haze at low latitudes (Finkbeiner 2004; Dobler & Finkbeiner 2008) and share their edges with the ROSAT X-ray map (Snowden et al. 1997). More recently, the Fermi bubbles are also found to be coincident with two giant radio lobes that appear to originate from the Galactic center (Carretti et al. 2013). These correlations found in the multi-wavelength observations seem to suggest that the Fermi bubble γ-rays (measured in the range of $\sim 1 - 100$ GeV) are produced by high-energy electrons via inverse Compton scattering of ambient low-energy photons, as the same electrons can also simultaneously produce radio synchrotron radiations in the presence of magnetic fields (Dobler et al. 2010). Moreover, the fact that the Fermi bubbles are well symmetric across the Galactic plane and also well centered on the Galactic center encourages to assume the bubbles, and also the associated γ-ray emission, to have their origin at the Galactic center (Su et al. 2010).

However, because of severe radiative losses, it would be extremely difficult to transport high-energy electrons from the Galactic center to the far edges of the bubbles. For electrons relevant for producing the Fermi bubble γ-rays, convection by Galactic wind would require a wind speed as high as $\sim 10^4$ km s^{-1} which is more than an order of magnitude larger than the typical Galactic wind speed of $\sim 200 - 300$ km s^{-1}, and diffusive transport would need a diffusion coefficient which is $\sim 2 - 3$ orders of magnitude larger than the standard Galactic value. This problem can be overcome using models based on jet activity of the central active galactic nucleus where jet speeds of over 10^4 km s^{-1} is readily achievable (Guo & Mathews 2012; Yang et al. 2012). An alternative solution would also be to consider production of electrons inside the bubbles itself, for instance, by generating multiple shock waves by periodic star capture by the central supermassive black hole (Cheng et al. 2011) or by second-order Fermi acceleration by the plasma wave turbulence present throughout the volume of the bubbles (Mertsch & Sarkar 2011).

On the other hand, models based on the π^0-decay origin of γ-rays suffer less constraint at least from the particle injection point of view. It has been shown that if cosmic-ray nuclei from the Galactic center are injected into the bubbles by fast wind of speed $\sim 10^3$ km s^{-1}, and if the cosmic rays remain trapped inside the bubbles for over $\sim 10^{10}$ yr, then the inelastic collisions of cosmic rays with the low-density bubble plasma, producing π^0 and $\pi^\pm$ mesons, can explain both the observed γ-rays and the radio emissions (Crocker & Aharonian 2011). In almost all the models proposed so far (see Su et al. 2010 for more scenarios), an additional process of high energy particle production, either inside or outside the bubble, has been considered in order to explain the observed γ-rays. In this letter, we present a "minimal" model which does not invoke any additional sources or particle production processes other than the sources responsible for the production of bulk of the Galactic cosmic rays.

In our model, it is assumed that cosmic rays (considered mainly as protons), after leaving their sources, undergo diffusive propagation through the Galaxy. If the Fermi bubbles are absent of sources, the diffusive streaming of cosmic rays in the direction of density gradient can result into a net flux of cosmic rays injected into the bubbles. Inside the bubbles, cosmic rays suffer losses due to inelastic collisions with the bubble plasma which, in steady state, is assumed to balance the injected flux. If the injection is uniform throughout the surface of the

s.thoudam@astro.ru.nl

bubbles, the total amount of cosmic-ray energy injected into each bubble per unit time (assuming spherical shape based on their projected images shown in Su et al. 2010) is given by $L = 4\pi R^2 u\varepsilon$, where R represents the radius of the bubble, u the streaming or injection velocity and ε the energy density of cosmic rays. For cosmic rays streaming at Alfvén velocity $v_A \sim 10^7$ cm s^{-1} which is the maximum streaming velocity in the case of scattering by self-generated Alfvén waves, the total cosmic-ray power injected is calculated to be $L \sim 4 \times 10^{40}$ ergs s^{-1} for $R = 4.5$ kpc and $\varepsilon = 1$ eV cm^{-3}, the locally measured cosmic-ray energy density. This amount of injected power is ~ 2 orders of magnitude larger than the power required in cosmic-ray protons to produce the measured γ-ray luminosity of $\sim 2 \times 10^{37}$ erg s^{-1} from each bubble. Even if the cosmic-ray density in the halo is lower by one order of magnitude with respect to the local value, this rough estimate shows that the injection of some fraction of Galactic cosmic rays into the bubbles can easily account for the measured γ-ray luminosity.

For cosmic rays with an equilibrium number density N_g in the Galaxy and propagating with diffusion coefficient D_g, their injected flux into the bubbles is given by $F_{inj} = D_g \nabla N_g \propto D_g N_g$, calculated at the edges of the bubbles. Since N_g is related to the cosmic-ray source spectrum Q as $N_g \propto Q/D_g$, we get $F_{inj} \propto Q$. Thus, cosmic rays streaming into the bubbles will follow the same spectral shape as the source cosmic-ray spectrum in the Galaxy.

Once injected, cosmic rays are assumed to undergo diffusive propagation inside the bubbles. If the plasma inside the bubbles is extremely turbulent as suggested by X-ray observations of the Galactic bulge (Yao & Wang 2007) or if the magnetic field lines are highly tangled (McQuinn & Zaldarriaga 2011), then the injected cosmic rays can take a considerable amount of time to penetrate the bubbles due to much slower diffusion. The longer cosmic rays take to penetrate, the more they can be affected by inelastic collisions with the bubble plasma resulting into depletion of density towards the center of the bubble. Such a density profile is also suggested by observations at low energies. The uniform projected intensity distribution of γ-rays observed from the Fermi bubbles seem to imply a non-uniform γ-ray emissivity distribution that peaks towards the edge (Su et al. 2010). Moreover, for a diffusion coefficient that scales with energy, the steady state cosmic-ray spectrum is expected to be close to $N_b \propto F_{inj} \propto Q$ near the boundary, and flatter towards the center. This is important because for the hadronic origin of Fermi bubble γ-rays, the γ-ray spectrum should mimic the spectrum of the bubble cosmic rays. The observed γ-ray spectral index of $\sim 2.0 - 2.1$ above ~ 1 GeV (Su et al. 2010) is slightly smaller than the cosmic-ray source index of $\sim 2.1 - 2.3$ required to produce the locally observed cosmic-ray spectrum.

2. MODEL CALCULATIONS

2.1. *Cosmic-ray spectrum*

In the absence of sources, the steady state distribution of cosmic-ray protons inside a bubble can be described by the diffusion-loss equation:

$$\nabla \cdot (D_b \nabla N_b) - \frac{N_b}{\tau} = 0 \tag{1}$$

where $N_b(\mathbf{r}, E)$ represents the differential number density of cosmic rays, E is the kinetic energy, D_b represents the diffusion coefficient inside the bubble, $\tau(E) = 1/(n_b v \sigma)$ represents the inelastic collision time with the bubble plasma of density n_b, v the velocity of cosmic rays and $\sigma(E)$ the inelastic collision cross-section (Kelner et al. 2006). In spherical symmetry, Eq. (1) reduces to the modified spherical Bessel differential equation as,

$$x^2 \frac{d^2 N_b}{dx^2} + 2x \frac{dN_b}{dx} - x^2 N_b = 0 \tag{2}$$

where we have written $x = r/\sqrt{\tau D_b}$ with r representing the radial variable. The solution of Eq. (2) is readily available as,

$$N_b(x, E) = \frac{A}{x} \sinh(x) + \frac{B}{x} e^{-x} \tag{3}$$

The second term of the solution can be neglected as it blows up at the center of the bubble ($r = 0$), and the constant A can be determined using the flux continuity relation at the bubble boundary $r = R$,

$$D_b \frac{dN_b}{dr}\bigg|_{r=R} = D_g \frac{dN_g}{dr}\bigg|_{r=R} \tag{4}$$

where the right hand side represents the flux of Galactic cosmic rays injected through the surface of the bubble F_{inj}. The final solution of Eq. (1) is then obtained as,

$$N_b(x, E) = F_{inj} \left(\frac{R}{x D_b}\right) \frac{\sinh(x)}{[\cosh(X) - \sinh(X)/X]} \tag{5}$$

where $X = R/\sqrt{\tau D_b}$.

To estimate F_{inj}, we write the Galactic cosmic-ray density as a function of perpendicular distance z to the Galactic plane as (Thoudam 2008),

$$N_g(z, E) \propto \frac{Q(E)}{D_g(E)} f_1(z) \tag{6}$$

where $Q(E)$ represents the source spectrum, and $D_g = 2.9 \times 10^{28} (E/E_0)^a$ cm^2 s^{-1} is the diffusion coefficient in the Galaxy with $E_0 = 3$ GeV and $a = 0.6$ (Thoudam 2008). The function

$$f_1(z) = \int_0^\infty \frac{\sinh[K(H - z)] \times \mathrm{J}_1(K\Re) dK}{\sinh(KH)\,[K \coth(KH) + \eta v \sigma/(2D_g)]} \tag{7}$$

has a very weak energy dependence, where J_1 is the Bessel function of order 1, H represents the halo boundary taken to be large enough to contain the Fermi Bubbles, $\Re$ the radial size of the source distribution taken as 20 kpc and η the averaged surface density of interstellar gas in the Galactic plane. Eq. (6) assumes that both the sources and the interstellar gas are uniformly distributed in the Galactic plane. In terms of the local density $N_g^0(E)$ which is taken to be at $z = 0$, Eq. (6) can be expressed as,

$$N_g(z, E) = \frac{N_g^0(E)}{f_2} f_1(z) \tag{8}$$

where,

$$f_2 = \int_0^\infty \frac{\mathrm{J}_1(K\Re) dK}{[K \coth(KH) + \eta v \sigma/(2D_g)]} \tag{9}$$

is also almost independent of energy. The cosmic-ray density gradient along z is then given by,

$$\frac{dN_g}{dz} = \frac{N_g^0(E)}{f_2}\frac{df_1}{dz} = CN_g^0(E) \quad (10)$$

where $C = (\nabla f_1)/f_2$, hereafter referred to as the injection coefficient, will determine the amount of Galactic cosmic rays injected into each bubble and depends on the distance z. In general, C may vary for different positions and also for different directions in the Galaxy. But, for the present study, we neglect variations in C and assume uniform cosmic-ray injection over the surface of the bubbles. We then treat C as a parameter which will be determined based on the measured γ-ray data. From Eq. (10), it can be noticed that as $N_g^0(E) \propto Q(E)/D_g(E)$,

$$D_g\frac{dN_g}{dz} \propto Q(E) \quad (11)$$

Eq. (11) shows that the flux of Galactic cosmic rays entering the bubbles $F_{inj} = D_g\nabla N_g\mid_{r=R}$ follows the source cosmic-ray spectrum in the Galaxy as mentioned before. We further assume that the diffusion coefficient inside the bubble scales with the galactic value as $D_b = KD_g$, where $K \ll 1$ is a constant. And, the cosmic-ray source index is taken to be $\Gamma = 2.2$ so that, for the assumed D_g, the demodulated local cosmic-ray intensity $(v/4\pi)N_g^0$ reproduces the measured proton spectrum between $\sim$ 10 GeV and 1000 GeV (Adriani et al. 2011).

2.2. *Gamma-ray emission*

In the present model, γ-rays from the bubbles are considered as the decay product of π^0 mesons produced from the inelastic collision of cosmic rays with the bubble plasma. For a constant plasma density inside the bubbles, the γ-ray emissivity is expected to follow the distribution of cosmic rays. The γ-ray emissivity as a function of the bubble radius is calculated using

$$q_\gamma(r, E_\gamma) = 2\int_{E_{\pi^0}^{min}}^{\infty}\frac{q_{\pi^0}(r, E_{\pi^0})}{\sqrt{E_{\pi^0}^2 - m_{\pi^0}^2}}dE_{\pi^0} \quad (12)$$

where E_γ denotes the γ-ray energy, E_{π^0} and m_{π^0} denote the total and the rest mass energy of the pion respectively, and $E_{\pi^0}^{min} = E_\gamma + m_{\pi^0}^2/4E_\gamma$. The π^0 mesons emissivity is given by (Kelner et al. 2006)

$$q_{\pi^0}(r, E_{\pi^0}) = \frac{\tilde{n}}{\tilde{k}}cn_b\sigma(T)N_b(r, T) \quad (13)$$

where c is the velocity of light, and $N_b(r, T)$ is the radial dependent cosmic-ray proton density given by Eq. (5) but taken as a function of the total energy T which is related to the pion energy as $T = m_p + E_{\pi^0}/\tilde{k}$. Following Kelner et al. (2006), we take $\tilde{k} = 0.17$, $\tilde{n} = 1$, and

$$\sigma(T) = \left(34.3 + 1.88L + 0.25L^2\right)\left[1 - \left(\frac{T_{th}}{T}\right)^4\right]^2 \text{ mb} \quad (14)$$

where $L = \ln(T/1\text{ TeV})$ and $T_{th} = 1.22$ GeV is the threshold energy for π^0 meson production.

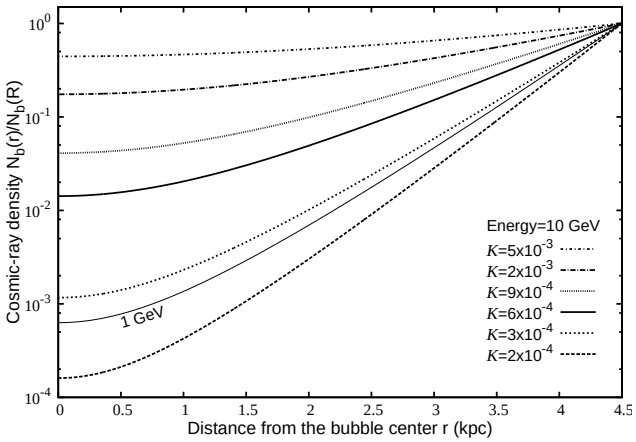

FIG. 1.— Normalized distribution of 10 GeV cosmic rays inside a Fermi bubble for different values of D_b with $K = (0.2 - 5) \times 10^{-3}$ and $n_b = 0.01$ cm^{-3}. The thin solid line is for 1 GeV particles for the case of $K = 6 \times 10^{-4}$.

The γ-ray intensity in a given direction characterized by the Galactic longitude l and the latitude b is calculated as

$$I_\gamma(l, b, E_\gamma) = \frac{1}{4\pi}\int_{y_1}^{y_2} q_\gamma(y, E_\gamma)dy \quad (15)$$

where the integration is performed along the line of sight distance y, and the integration limits are determined from the points of intersection of the line of sight with the bubble surface. In calculating Eq. (15), the emissivity previously calculated as function of the bubble radius r has been carefully expressed as function of y.

3. RESULTS AND DISCUSSIONS

The distribution of cosmic rays inside the bubbles is governed by the competition between diffusion and inelastic collision. Diffusion tends to uniform the distribution while inelastic collision does the opposite by removing particles. A slow diffusion process will be more affected by inelastic collisions, leading to more exclusion of cosmic rays from the bubble interiors. Thus, faster diffusion will produce more uniform distribution than slower diffusion.

For energies of our interest, the inelastic collision crosssection is known quite accurately and hence, for a given plasma density, the inelastic collision time $\tau(E)$ can be fixed. On the other hand, the diffusion coefficient inside the bubbles is largely unknown although a value smaller than the Galactic averaged is suggested (Yao & Wang 2007). Figure 1 shows the normalized distribution of 10 GeV cosmic rays (thick lines) inside a bubble for different values of D_b with $K = (0.2 - 5) \times 10^{-3}$ taking $n_b = 0.01$ cm^{-3} (Su et al. 2010). It can be seen that the distribution becomes flatter towards the center of the bubble as K takes larger values which is due to the shorter diffusion times $t \sim R^2/D_b$ of cosmic rays to reach the center. Also shown for comparison is the distribution of 1 GeV particles (thin solid line) for the case of $K = 6 \times 10^{-4}$. The distribution is steeper than the corresponding distribution of 10 GeV particles (thick solid line). In our model, the cosmic-ray distribution is expected to be more uniform at higher energies due to the energy scaling of the diffusion coefficient as $D_b \propto E^{0.6}$.

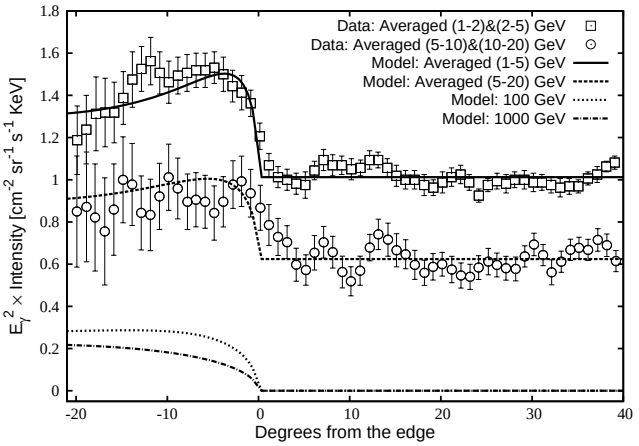

FIG. 2.— Projected γ-ray intensity profile of the Southern bubble for the averaged $1-5$ GeV (solid line) and $5-20$ GeV (dashed line). Also shown are the predictions for 100 GeV (dotted line) and 1000 GeV (dot-dashed line) energies. Data are taken from Su et al. (2010).

Once the value of τ is fixed, the cosmic-ray distribution inside the bubbles is determined by the choice of D_b (through the constant parameter K). Here, its value is chosen such that the resulting projected γ-ray intensity distribution matches the measured profile. It is found that choosing $K = 2.2 \times 10^{-4}$ produces a good fit to the measured data as shown in Figure 2, where the data represents the measurements from the Southern bubble. The calculation assumes $R = 4.5$ kpc and the bubble center to be at 5 kpc above the Galactic center (Su et al. 2010). The model predictions for both the averaged $1-5$ GeV (solid line) and $5-20$ GeV (dashed line) are added with backgrounds obtained by fitting horizontal lines to the respective data between 5° and 40°. It can be mentioned that neither the hadronic model presented in Crocker & Aharonian (2011) nor the leptonic model based on diffusive shock acceleration (Cheng et al. 2011) can satisfactorily explain the measured sharp edges shown in Figure 2. Both these models predicted a constant volume emissivity throughout the bubbles which will produce soft edges on the projected profile. Also shown in Figure 2 are the predictions for 100 GeV (dotted line) and 1000 GeV (dot-dashed line) γ-rays which can be tested in future. Their profiles are relatively steeper towards the edge than at low energies, and also show softer edges, reflecting the more uniform particle distribution at higher energies. It can be noted that our result at high energies, say at 1000 GeV, is clearly different from that expected from the leptonic stochastic acceleration model presented in Mertsch & Sarkar (2011) which predicted a significant edge brightening at high energies. This difference in the high energy radial profile can be used to differentiate between the two models in future.

The γ-ray spectrum averaged over a whole bubble is shown in Figure 3 (top). The calculation assumes $\Gamma = 2.2$ as mentioned before and an injection coefficient of $C = 4.6 \times 10^{-3}$ kpc^{-1}. The latter corresponds to an injection flux of 0.46% of the local cosmic-ray density injected with velocities of $\sim 10^7$ cm s^{-1} at few GeVs into each bubble. Note that this is also the same injection strength used to produce the results presented in Figure 2. The model prediction is found to be in good agreement with the data in the energy range of $\sim 1-100$ GeV where the

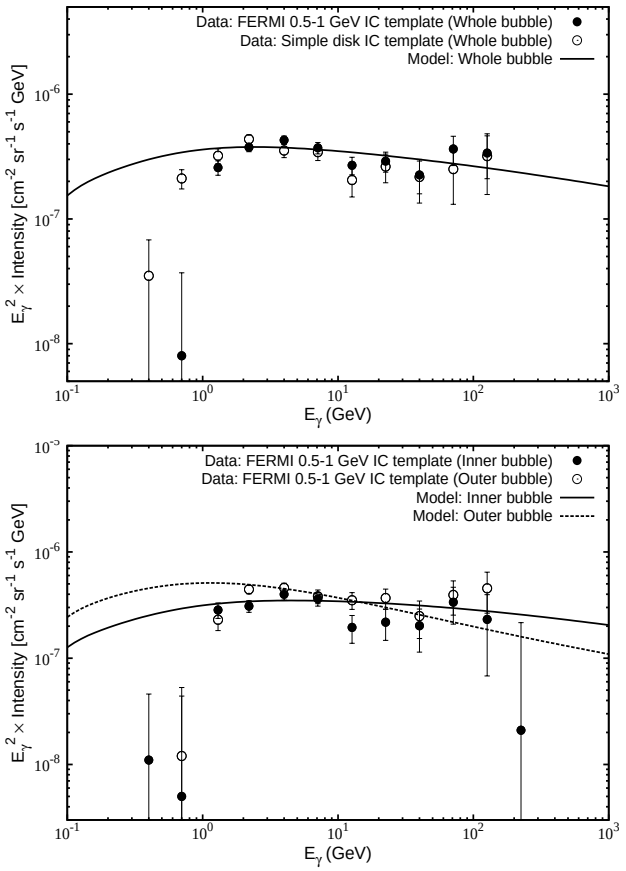

FIG. 3.— Gamma-ray spectra for a whole bubble (top), and for the bubble inner and outer regions (bottom). The outer region is taken as a shell of 1 kpc thickness. Data are from Su et al. (2010).

measurement uncertainties are small. It is interesting to see that the same source index required to explain the measured cosmic-ray spectrum also reproduces the Fermi bubble γ-ray spectrum.

Spectra for the inner and outer regions of a bubble separated as in Su et al. (2010) are shown in Figure 3 (bottom). The outer region is taken as a shell with thickness 1 kpc. The present model produces a steeper γ-ray spectrum in the outer region than in the inner region. For the inner, the model prediction agree nicely with the measured data between $\sim 1-100$ GeV, but for the outer region, the model spectrum seems to be somewhat steeper compared to the data. Choosing a smaller diffusion index inside the bubble will produce more spectral uniformity in the two regions. However, for any reasonable value of the diffusion index, our model prediction is expected to be different from that of the leptonic model (Mertsch & Sarkar 2011) in which a steeper spectrum in the inner region is expected.

In our calculations so far, we have assumed that the cosmic-ray diffusion index inside the bubbles is the same as that in the Galaxy. It is possible that the index is different in the two regions depending on the nature of the turbulent wave responsible for scattering the cosmic-rays. Actually, a higher turbulent region is expected to have a steeper turbulent wave spectrum $w(k) \propto k^{-\alpha}$ (where k represents the wave number) which then translates into a flatter diffusion index. For a Kolmogorov type wave spectrum which is characterized by a turbulent index of

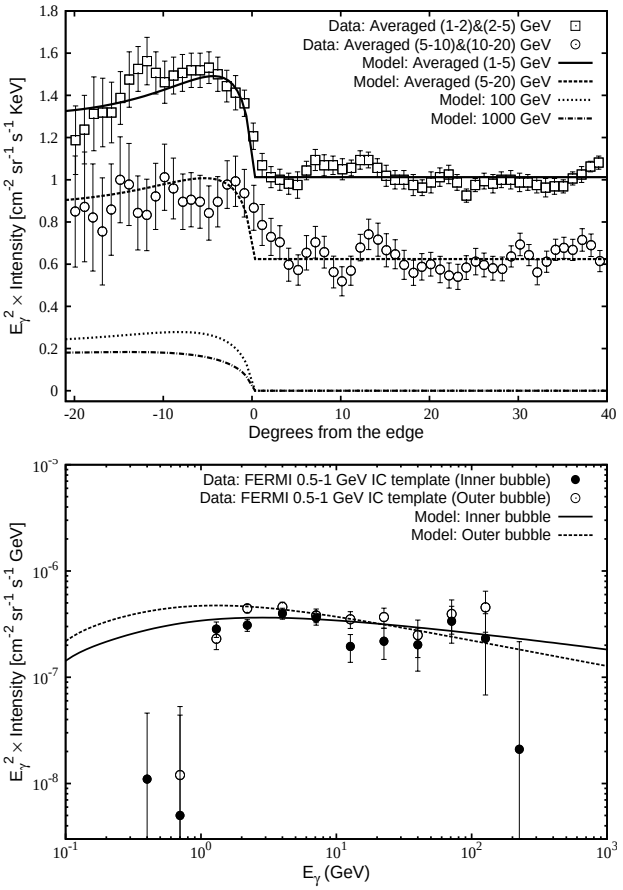

FIG. 4.— Same as Figure 2 and Figure 3 (bottom panel), but for $D_b \propto E^{1/3}$ and $K = 5.5 \times 10^{-4}$.

$\alpha = 5/3$, the diffusion index becomes $a = 1/3$. We have also carried out calculations taking $a = 1/3$ inside the bubbles (keeping $a = 0.6$ for the region outside). For the same value of injection coefficient obtained above for the case of $a = 0.6$, it is found that a value of $K = 5.5 \times 10^{-4}$ is required in order to explain both the measured intensity radial profile and the measured spectrum simultaneously. The results are shown in Figure 4. For the radial profile, noticeable changes are observed only at high energies. For instance, the profile for 1000 GeV becomes comparatively flatter with shaper edges than the corresponding result shown in Figure 2 for the case of $a = 0.6$. At low energies, the radial profiles look very much similar in the two cases. Also, from Figure 4 bottom panel, it can be noticed that the difference in the predicted spectra between the inner and outer regions of the bubble becomes less. Thus, more sensitive spectral measurements at high energies can give a better constrain on the diffusion index in the present model.

It should be mentioned that although our simple model can successfully explain the observed radial profiles for the Southern bubble, it cannot explain the dip at $\sim -12^\circ$ observed in the $5-20$ GeV profile of the Northern bubble (Su et al. 2010). Moreover, also the apparent hardening of the observed spectrum below ~ 1 GeV cannot be satisfactorily explained (see Figures 3 and 4 bottom). So far, none of the existing models can explain this spectral behavior. Future accurate measurement of this low-energy spectral shape will be crucial for better understanding the nature of high-energy particles responsible for the γ-ray emission.

4. CONCLUSIONS

In this letter, we have proposed a minimal model for the Fermi bubbles which, unlike other existing models, does not consider any additional particle production processes or sources other than those responsible for the production of the Galactic cosmic rays. The model considers that the γ-rays from the bubbles can be the result of injection of Galactic cosmic-ray protons during their diffusive propagation through the Galaxy. It is found that this simple model can explain many of the observed properties of the Fermi bubbles.

I wish to thank D. Jones and A. Achterberg for insightful discussions. I also thank J. R. Hörandel, H. Falcke, and P. Groot for constant encouragement.

REFERENCES

Adriani, O., et al. 2011, Science, 332, 69
Carretti, E., et al. 2013, Nature, 493, 66
Cheng, K. S., et al. 2011, ApJL, 731, L17
Crocker, R. M., & Aharonian, F., 2011, PRL, 106, 101102
Dobler, G., & Finkbeiner, D. P., 2008, ApJ, 680, 1222
Dobler, G., et al. 2010, ApJ, 717, 825
Finkbeiner, D. P., 2004, ApJ, 614, 186
Guo, F., & Mathews, W. G., 2012, ApJ, 756, 181
Kelner, S. R., Aharonian, F. A., & Bugayov, V. V., 2006, PRD 74, 034018
McQuinn, M., & Zaldarriaga, M., 2011, MNRAS, 414, 3577
Mertsch, P., & Sarkar, S., 2011, PRL, 107, 091101
Snowden, S. L., et al. 1997, ApJ, 485, 125
Su, M., Slatyer, T. R., & Finkbeiner, D. P., 2010, ApJ, 724, 1044
Thoudam, S. 2008, MNRAS, 388, 335
Yang, H.-Y. K., et al. 2012, ApJ, 761, 185
Yao, Y., & Wang, Q. D., 2007, ApJ, 666, 242